



Corrosion Mitigation of Carbon Steel in Acidic Media Using Glimepiride: A Sulfonylurea Derivative as an Eco-Friendly Inhibitor

Samir Abd El Maksoud¹, Abd El Aziz Fouda², Haby Badawy^{1,*}

¹ Department of Chemistry, Faculty of Science, Port Said University, Port Said, Egypt.

² Department of Chemistry, Faculty of Science, Mansoura University, Mansoura-35516, Egypt

*Corresponding author: habybadawy@gmail.com

ABSTRACT

This study investigates the effectiveness of expired Glimepiride drug, a sulfonylurea derivative, as a corrosion inhibitor for carbon steel (CS) degrading in 1.0 M hydrochloric acid solutions. Experimental and theoretical procedures examine glimepiride inhibition efficiency as Weight loss (WL) measurements, electrochemical techniques (potentiodynamic polarization (PP), electrochemical frequency modulation (EFM), and electrochemical impedance spectroscopy (EIS)) and surface characterization methods (Fourier transform infrared spectroscopy (FTIR), atomic force microscopy (AFM), scanning electron microscopy (SEM), and X-ray photoelectron spectroscopy (XPS)) were employed. The inhibition efficiency increased with both rising inhibitor concentration and increasing temperature (303–318 K). Adsorption studies indicated that the inhibitors followed the Temkin isotherm, with thermodynamic and kinetic parameters suggesting a chemical adsorption. glimepiride act as mixed type inhibitor as a result from electrochemical techniques. SEM and XPS studies revealed that the inhibitor was adsorbed on the surface of carbon steel, resulting in a considerable reduction in corrosion rate. Theoretical calculations gave useful information on Glimepiride's molecular characteristics, supporting experimental findings that Glimepiride acts as a corrosion inhibitor.

Keywords: Glimepiride, Corrosion inhibition, Electrochemical, Impedance, Carbon steel.

1. INTRODUCTION

Corrosion of metallic structures is a serious concern in many industries, affecting production costs, safety measures, and the environment [1-6]. The necessity to repair and replace rusted components causes economic losses and production delays [7]. As a result, proactive actions are required during the design process to address corrosion-related concerns [8]. The petroleum, water, gas, paper, chemical, and power generation industries are highly sensitive to corrosion [9-12]. Corrosion not only increases production

costs but also depletes natural resources [13]. As a result, metallic materials used in these industries must be strong corrosion resistant [14]. Carbon steel is widely used in a variety of industrial applications due to its strong passive coating and excellent corrosion resistance [15,16]. It is especially well-suited for corrosive environments found in offshore oil, gas, and other industries due to its remarkable mechanical qualities and resistance to corrosion [17]. Economic factors related to corrosion-induced expenses, the necessity of conserving natural resources, and energy usage during material manufacture and extraction are only a few of the many aspects that make up corrosion research [18]. Corrosion mitigation techniques have therefore attracted a lot of study attention [19]. In order to reduce the corrosion of metallic components, corrosion inhibitors have become an essential in metal protection [20–23]. The longevity of the material is increased by these inhibitors, which work by slowing down the deterioration process. They accomplish this by preventing and postponing corrosive processes and creating a protective layer on the metal's surface [24–26]. The using of synthetic chemical inhibitors has decreased due to worries about environmental regulations, human and wildlife health risks, and their toxicity [27–29]. As a result, several studies are interested in investigating long-lasting and extremely strong environmentally safe inhibitors. [30–32]. These desirable substitutes should be affordable, non-toxic, extremely effective, adaptable, eco-friendly, and safe to disposed of. Furthermore, a protective coating is formed as a result of the inhibitor's strong attachment to the metal's exterior surface due to the covalent adsorption between nitrogen-positive ions and the metal surface. Superior corrosion inhibition capability is achieved by this coating's efficient prevention of contact between corrosive media and metal surfaces. The purpose of this study is to use direct experimental methods to understand the effectiveness of Glimepiride as a corrosion inhibitor for carbon steel in 1.0 M hydrochloric acid. Weight loss (WL), electrochemical methods, surface analyses, and theoretical computations are some of the validation approaches used in this work.

2. RESOURCES AND PROCEDURES

2.1 RESOURCES

Table 1 Composition of CS employed in this study.

C	Mn	P	Si	Cr	N	S	Cu	Fe
0.14	0.52	0.05	0.02	0.03	0.02	0.04	0.02	Rest

A 35% hydrochloric acid solution was employed to prepare the degradative medium (1.0 M).

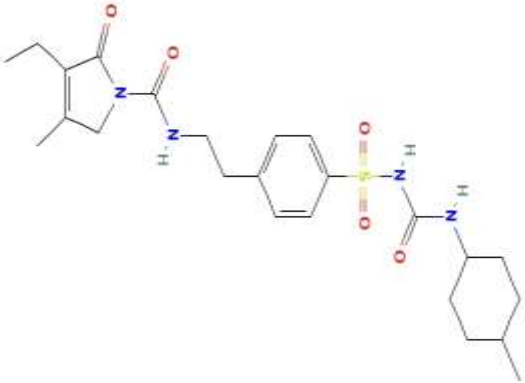
Preparation stock solution (1000 ppm):

The calculated weight of Glimepiride powder was first dissolved in 20 mL of DMSO (Dimethyl Sulfoxide) to complete dissolution, then diluted with bi-distilled water till reach a 1000 mL solution.

Preparation working solutions:

From the 1000 ppm stock solution, the concentrations ranged from (50-300 ppm) were prepared by serial dilution using bi-distilled water to 100 mL total volume.

Table 2: Molecular configurations, nomenclature, and chemical composition of Glimepiride

Configuration	Nomenclature	chemical Composition
 <p style="text-align: center;">3.</p>	<p>1-[[4-(2-[[[3-ethyl-4-methyl-2-oxo 2,5-dihydro-1H-pyrrol-1-yl]carbonyl] amino] ethyl) phenyl]sulfonyl]-3-(trans-4-methyl cyclohexyl)urea</p>	$C_{24}H_{34}N_4O_5S$

2.2. PROCEDURES

2.2.1 WEIGHT LOSS EXAMINATION

Seven specimens of CS with the dimensions of 2 cm x 2 cm x 0.1 cm were utilized. The specimens underwent a systematic surface preparation process using sandpaper of progressively finer grades (400, 800, and 1200 grit), until a mirror-like finish was achieved. followed by degreasing with acetone and rinsing with bidistilled water, dried, and their mass was recorded. Glimepiride solutions of varying concentrations were prepared in a 100 ml solution of 1.0 M hydrochloric acid. A control solution without Glimepiride was also prepared. The (CS) specimens were then immersed in the prepared Glimepiride solutions for specific time intervals of 30, 60, 90, 120, 150, and 180 minutes. After each immersion interval, the specimens were removed, rinsed with bidistilled water, dried, and their mass was re-measured. The inhibition efficiency (IE%) and surface coverage (θ) was calculated using Equation (1) [33]:

$$IE\% = \left(1 - \left[\frac{W}{W_0} \right] \right) \times 100 = \theta \times 100 \quad (1)$$

We represents mass loss for CS without Glimepiride and W represent mass loss with Glimepiride.

2.2.2 ELECTROCHEMICAL PROCEDURES

Potentiodynamic polarization (PP), electrochemical impedance spectroscopy (EIS), and electrochemical frequency modulation (EFM) techniques were used to investigate the corrosion behavior of carbon steel (CS). A three-electrode glass cell system was used, consisting of a saturated calomel electrode (SCE) as a reference electrode, a platinum electrode as a counter electrode, and a CS electrode (1 cm²) as a working electrode.

Before each experiment, the CS electrode was subjected to a uniform surface preparation technique. This entailed polishing with several grades of sandpaper (400, 800, and 1200 grit), then degreasing with acetone and rinsing with bidistilled water. The electrode was then dried on filter paper. The open circuit potential (OCP) was measured and recorded for 30 minutes until a steady-state condition was reached.

2.2.2.1. P.P PROCESSES

Tafel graphs were generated by automatically adjusting the sweep potential from -0.750 to -0.250 V, with scan rate of 1 mV//s. The corrosion current density was evaluated, and the inhibition efficiency and surface coverage were estimated by Equation (2) [34]:

$$IE\% = \left(1 - \left[\frac{i_{\text{corr(inh.)}}}{i_{\text{corr(free)}}} \right] \right) \times 100 = \theta \times 100 \quad (2)$$

Where $i_{\text{corr(free)}}$ represents corrosion current densities without Glimepiride, $i_{\text{corr(inh.)}}$ with Glimepiride.

2.2.2.2. EIS PROCESSES

Impedance measurements were performed in the frequency range of 100 KHz to 0.1 Hz with an amplitude of 5 mV. Equation (3) calculates IE% and θ using (EIS) data [35]:

$$IE\% = \left(1 - \left[\frac{R_{\text{ct}}}{R_{\text{ct}}^{\circ}} \right] \right) \times 100 = \theta \times 100 \quad (3)$$

Where R_{ct}° represents the charge transfer resistances in absence of Glimepiride, R_{ct} in presence of Glimepiride.

The double layer capacitance (C_{dl}) values in various concentrations were determined by Eq. (4) [41]:

$$C_{\text{dl}} = \frac{1}{2\pi f_{\text{max}} R_{\text{ct}}} \quad (4)$$

Where f_{max} represent the value of maximum frequency.

2.2.2.3 EFM PROCESSES

EFM approach serves as quick and efficient method for evaluating the degradation of carbon steel without the necessity of determining the Tafel slopes. EFM was achieved using signal amplitudes of 10 mV and 2 sine wave frequencies of 2 and 5 Hz. primary focus was on identifying causality coefficients (CF-2 & CF-3), corrosion current density (i_{corr}), and Tafel slope (β_c & β_a) [37].

2.2.3. SURFACE PROCESSES

A series of assays were conducted to investigate the outer layer morphology of CS after exposure to a degradative solution containing 300 ppm of Glimepiride for 24 hours at 25°C . The surface roughness of the CS was assessed using atomic force microscopy (AFM), specifically with a Thermo Fisher Nicolet IS10 scanning probe microscope. The binding energies of various bonds present on the CS surface were determined using X-ray photoelectron spectroscopy (XPS), which was performed using the K-ALPHA instrument from Thermo Fisher Scientific (USA). Furthermore, Fourier-transform infrared (FTIR) spectra of pure solutions of Glimepiride and CS were obtained using a PerkinElmer 1600 spectrophotometer.

2.2.4 SIMULATION PROCESSES

MSD Mol440 identified quantum chemical indicators using density functional theory (DFT) [38]. The indicators calculated for Glimepiride included softness (σ), molecular polarity (μ), electronegativity (X), ionization potentials (I), lowest unfilled molecular orbital (E_{LUMO}), hardness (η), energy gap (ΔE), and highest filled molecular orbital (E_{HOMO}).

3. RESULTS AND DISCUSSION

3.1. WEIGHT LOSS (WL) TEST

3.1.1. GLIMEPIRIDE CONCENTRATION EFFECT

Figure 1 shows the decrease in mass loss in the case of the addition of different concentrations of Glimepiride compared with the case of exposure to one molar hydrochloric acid with and without Glimepiride. Table 3 indicates that an increase in the concentration of Glimepiride led to an increase in inhibition efficiency (IE%) due to the formation of a protective layer by Glimepiride on the outer surface of CS. This layer reduced the dissolution of the metal, resulting in lower weight loss and a reduced degradation rate [39]. Figure 2 show that IE% increases gradually during time (0–120 minutes), which can be attributed to the adsorption of Glimepiride molecules on carbon steel surface. This indicate that the formation of the protective layer is time-dependent, and the surface coverage improves by time increases. After approximately 120 minutes, the IE% tends to stabilize, indicating that the surface becomes saturated with inhibitor molecules, and a stable protective layer is established.

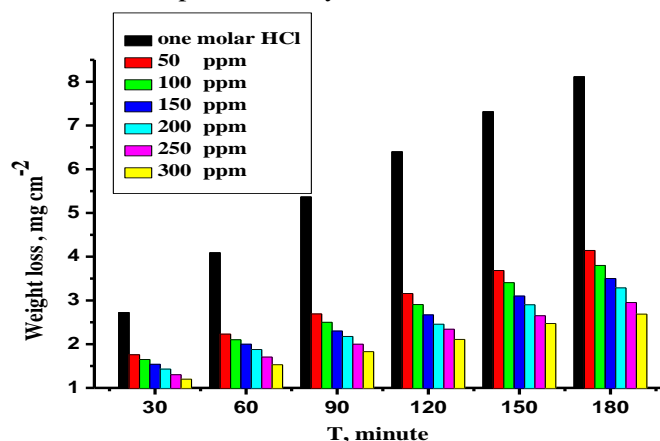


Figure 1: Weight loss over time for the corrosion of CS in 1.0 M HCl both in varying concentrations of Glimepiride and in its nonexistence at 298 K.

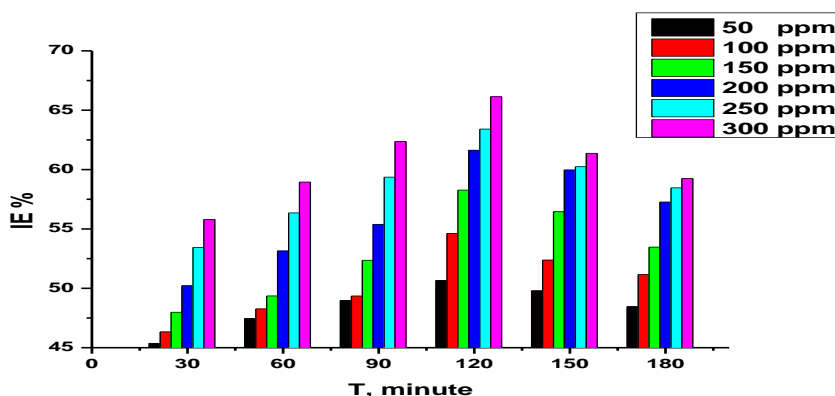


Figure 2: Inhibition efficiency (IE%) over time for CS in 1.0 M HCl in varying concentrations of Glimepiride at 289 K.

Table 3: The variation of mass loss, corrosion rate, and inhibition efficiency in the absence and presence of varying concentrations of Glimepiride at 120 min.

Concentration	Temperature	Weight loss	$k_{corr} \times 10^{-3}$	θ	% IE
Blank	298	6.4	53.33	-	-
50		3.15	26.30	0.506	50.6
100		2.90	24.20	0.546	54.6
150		2.67	22.25	0.582	58.2
200		2.45	20.46	0.616	61.6
250		2.34	19.51	0.634	63.4
300		2.16	18.05	0.661	66.1

3.1.2. TEMPERATURE EFFECT

The degradation rate of CS in 1.0 M HCl, along with varied doses of Glimepiride, is depicted in Table 4, indicating a rapid acceleration in the degradation rate within the aggressive solution. Figure 2 visually represents the impact of temperature on the inhibition efficiency at various Glimepiride doses when dissolving CS in a 1.0 M hydrochloric acid solution at different temperatures. The inhibition efficiency percentage increases as the temperature of the compound's solution rises, suggesting that Glimepiride chemically adsorbs on the surface of carbon steel [40].

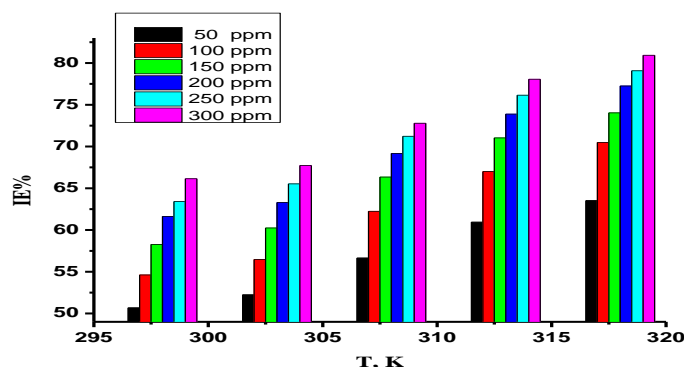


Figure 2: Temperature effect on the IE% for varied concentrations of Glimepiride.

Table 4: Weight loss values for carbon steel at 120 minute in the absence and presence of varying concentrations of Glimepiride at distinct temperatures

Concentration ppm	Temperature K	Weight loss	$k_{corr} \times 10^{-3}$ $mg\ cm^{-2}$	θ	IE%
Blank	303	7.01	58.42	-	-
50		3.34	27.90	0.522	52.2
100		3.05	25.43	0.564	56.4
150		2.78	23.22	0.602	60.2
200		2.57	21.44	0.632	63.2
250		2.41	20.13	0.655	65.5
300		2.26	18.85	0.677	67.7
Blank	308	9.62	80.1	-	-
50		4.17	34.76	0.566	56.6
100		3.63	30.27	0.622	62.2
150		3.23	26.97	0.663	66.3
200		2.96	24.71	0.691	69.1
250		2.76	23.06	0.712	71.2
300		2.61	21.81	0.728	72.8
Blank	313	12.82	106.8	-	-
50		5.00	41.73	0.609	60.9
100		4.23	35.26	0.669	66.9
150		3.71	30.95	0.710	71.0
200		3.34	27.89	0.738	73.8
250		3.05	25.48	0.761	76.1
300		2.81	23.43	0.780	78.0
Blank	318	15.42	128.5	-	-
50		5.62	46.88	0.635	63.5
100		4.55	37.92	0.704	70.4
150		4.00	33.36	0.740	74.0
200		3.50	29.22	0.772	77.2
250		3.22	26.89	0.790	79.0
300		2.94	24.50	0.809	80.9

3.1.3. ACTIVATION THERMODYNAMIC PARAMETERS

Arrhenius Eq. (5) [41-42]:

$$k_{corr} = A \exp(-E_a / RT) \tag{5}$$

Where A: Arrhenius constant, R : the gas constant, E_a^* : activation energy, k_{corr} : corrosion rate and T : absolute temperature.

Graph $\log k_{corr}$ vs. $1/T$ is represent by figure 3 where E_a^* is calculated and recorded in Table 5. Equation (6) represent the transition stat.

$$k_{corr} = (RT/Nh) \exp(\Delta S^*/R) \exp(-\Delta H^*/RT) \tag{6}$$

Where ΔS^* and ΔH^* are the entropy and enthalpy of activation. The relation between $\log k_{corr}/T$ vs. $1/T$ is represent by figure 4. ΔH^* and ΔS^* are calculated and tabulated in table 5. A chemical adsorption suggestion due to low values of E_a^* and an endothermic process of activation due ΔH^* positive values [43]. the activation energy (Ea) should increase in the presence of an effective physical inhibitor. This is because the adsorbed inhibitor molecules form a protective layer on the metal surface, so increasing the energy barrier for the corrosion reaction and slowing down the rate of metal dissolution. While lower (Ea) in the presence of the glimepiride could suggest a chemical adsorption (chemisorption) of the glimepiride molecules on carbon steel surface, which indicate a stronger and more stable interaction with the metal surface[44-48].

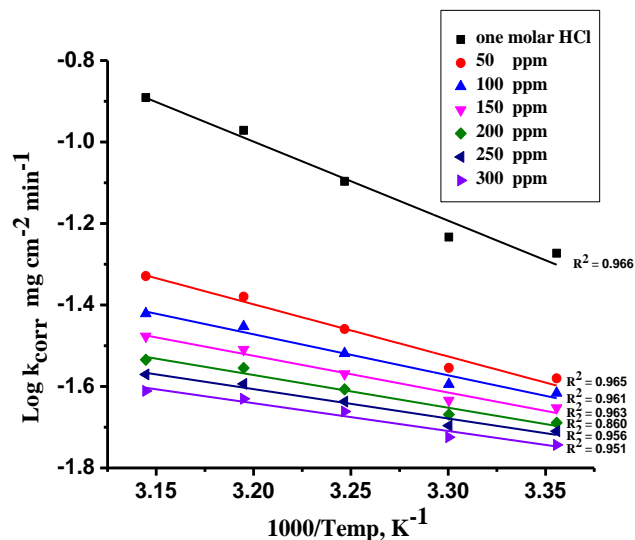


Figure 3. Carbon steel degradation in degradative acid solution Arrhenius graph both without plus with Glimepiride varying concentration at temperature ranging from (298-318K)

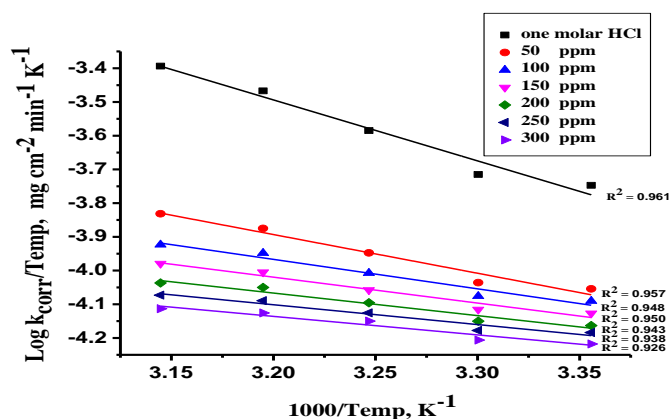


Figure 4. Log transition state without and with different concentrations from Glimepiride at temperature ranging from (298-318K)

Table 5: Thermodynamic activation without and with different concentrations from Glimepiride at temperature ranging from (298-318K)

Concentration ppm	E_a^* kJ mol^{-1}	ΔH^* kJ mol^{-1}	$-\Delta S^*$ $\text{J mol}^{-1}\text{K}^{-1}$
0.0	37.2	34.6	153.6
50	27.5	25.0	196.3
100	24.3	21.3	209.4
150	23.9	19.0	218.3
200	17.8	15.4	230.9
250	15.9	12.6	241.5
300	14.3	12.4	241.6

3.1.4. ADSORPTION ISOTHERMS

Inhibitor adsorption over metal surface is influenced by: (1) metal properties and charge, (2) inhibitor chemical structure and (3) electrolyte concentration [49]. By fitting the various adsorption isotherms including Freundlich, Temkin, Langmuir, Flory-Huggins and Henry isotherms, the data were tested graphically as shown in Table 6. The best fitted isotherms that describe the adsorption behavior of Glimepiride on CS surface was Temkin adsorption isotherm and it can be expressed by using the equation as described by Equation (7) , aligns well with the experimental data.

$$\theta = \left(\frac{2.303}{a}\right) \text{Log } K_{\text{ads}} + \left(\frac{2.303}{a}\right) \text{Log } C \tag{7}$$

Where, Surface coverage θ , adsorption constant K_{ads} , inhibitor concentration C and heterogeneous factor a . which have a positive value in case of attraction between Glimepiride and CS surface and negative value in cases of repulsion . The more attraction, the more inhibition.

Graphing θ over $\log C$ represent by figure 5 where a , K_{ads} and $\Delta G^{\circ}_{\text{ads}}$ calculated and recorded in Table 7. Indicated the adsorption isotherm follows Temkin model in a good manner.

Equation (8) calculate ($\Delta G^{\circ}_{\text{ads}}$), using K_{ads} in:

$$\Delta G^{\circ}_{\text{ads}} = -RT \ln (55.5 K_{\text{ads}}) \tag{8}$$

The significant adsorption of Glimepiride onto the CS surface is indicated by the notable increase in $\Delta G^{\circ}_{\text{ads}}$, which amounts to approximately -40 kJ/mol. The elevated values of K_{ads} at higher temperatures suggest a coordination between the active groups of Glimepiride and the unoccupied d-orbitals in CS, effectively inhibiting corrosion. The adsorption process is spontaneous, as indicated by the negative value [50].

Equation (9) calculate ($\Delta H^{\circ}_{\text{ads}}$) [51]:

$$\text{Log } K_{\text{ads}} = -\frac{\Delta H^{\circ}_{\text{ads}}}{2.303 RT} \tag{9}$$

Graphing $\text{Log } K_{\text{ads}}$ over $1/T$ represent by figure 6 where $\Delta H^{\circ}_{\text{ads}}$ calculated and recorded in table 7.

Equation (10) calculated ($\Delta S^{\circ}_{\text{ads}}$)

$$\Delta G^{\circ}_{\text{ads}} = \Delta H^{\circ}_{\text{ads}} - T\Delta S^{\circ}_{\text{ads}} \tag{10}$$

Values of $\Delta H^{\circ}_{\text{ads}}$ greater than 40 kJ/mol, with $\Delta S^{\circ}_{\text{ads}}$ around 100 kJ/mol indicate chemisorption and an endothermic process [52], showing the involvement of non-bonding electron pairs from Glimepiride atoms in interactions with the CS surface. A positive "a" value suggests that the adsorbed layers interact with the carbon steel surface, and the increase in K_{ads} with temperature demonstrates an improvement in the adsorption equilibrium at higher temperatures. Negative entropy values in table 7 indicate that Glimepiride adsorbs more than it desorbs onto the CS surface. The increasing $\Delta S^{\circ}_{\text{ads}}$ values in table 7 reflect greater disorder resulting from the adsorption of H_2O molecules facilitated by Glimepiride onto CS [53].

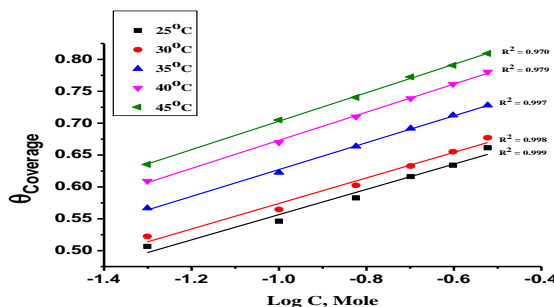


Figure 5. Surface coverage (θ) vs. Log C at different temperatures (298-318K)

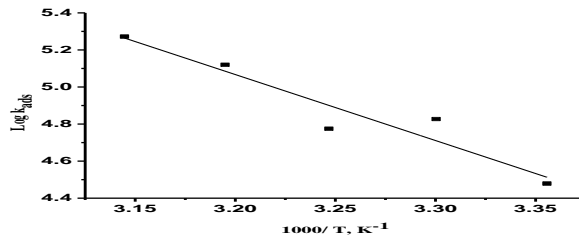


Figure 6 Glimepiride varying concentration adsorption onto carbon steel surface graphs Log Kads over 1/T at different temperatures (298-318K)

Table 6 Different isotherm adsorption data for Glimepiride onto CS surface in degradative acid solution at distinct temperature.

<p style="text-align: center;"> $\theta / 1 - \theta = K C$ Langmuir </p>	<p style="text-align: center;"> $a \theta = \ln K C$ $(a / 2.303) \theta = \log K + \log C$ $\theta = (2.303/a) \log K + (2.303/a) \log C$ Temkin </p>
<p style="text-align: center;"> $\theta = K C^n$ $\log \theta = \log K + n \log C$ Freundlich </p>	<p style="text-align: center;"> $\log \theta / C = \log K + \log (1 - \theta)$ Flory-Huggins </p>
	<p style="text-align: center;"> $\theta = K C$ Henry </p>

Table 7 Temkin isotherm adsorption data for Glimepiride onto CS surface in degradative acid solution at distinct temperature

Temperature K	Log K_{ads} , M^{-1}	a	$-\Delta G_{ads}^{\circ}$ $kJ mol^{-1}$	ΔH_{ads}° $kJ mol^{-1}$	$-\Delta S_{ads}^{\circ}$ $J mol K^{-1}$
298	4.212	11.5	35.0	51.8	117.9
303	4.351	12.3	37.4		123.8
308	4.484	12.1	37.9		123.4
313	4.756	13.4	40.0		128.1
318	4.995	14.1	41.5		133.0

3.2. ELECTROCHEMICAL PROCEDURES

3.2.1. P.P. PROCESSES

The behavior of CS polarization in degradative acid solution was examined, both with varying concentrations of Glimepiride and in its absence, as shown in figure 7. The resulting table (Table 8) records the anodic β_a Tafel slope, corrosion potential E_{corr} , cathodic β_c Tafel slope, surface coverage θ , inhibition efficiency IE%, and corrosion current density i_{corr} . The addition of Glimepiride led to a reduction in i_{corr} , indicating its effectiveness as a corrosion inhibitor with a mixed-type inhibition function, as inferred from the minimal changes observed in the Tafel slopes and E_{corr} [54]. Tafel plots, both with and without Glimepiride, suggest that the corrosion mechanism remains unchanged.

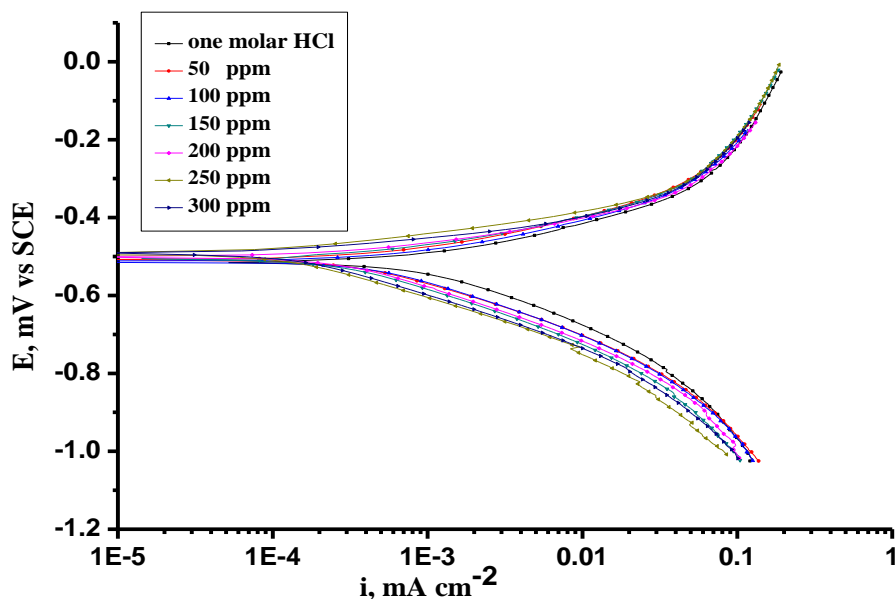


Figure 7: carbon steel degradation in degradative acid solution potentiodynamic polarization graph with varying concentration of Glimepiride

Table 8: values from the potentiodynamic polarization of carbon steel in degradative acid solution, both without plus with Glimepiride varying concentration

Concentration Ppm	$-E_{\text{corr}}$, mV vs. SCE	i_{corr} , $\mu\text{A cm}^{-2}$	$-\beta_c$, mV dec ⁻¹	β_a , mV dec ⁻¹	k_{corr} , mpy	R_p , $\Omega \cdot \text{cm}^2$	θ	IE%
0.0	533	1480	210	134	755	29.78	-----	-----
50	508	572	168	88	301	59.71	0.613	61.3
100	515	490	186	110	255	79.86	0.668	66.8
150	508	478	184	102	247	74.85	0.677	67.7
200	500	360	175	82	197	97.38	0.756	75.6
250	496	337	170	80	173	99.94	0.772	77.2
300	494	304	176	82	157	109.44	0.794	79.4

3.2.2. EIS PROCESSES

The electrical equivalent circuit corresponding to the observations depicted in figure 8 was utilized to analyze CS Nyquist plots in degradative acid solution. These plots depicted varying concentrations of Glimepiride and its absence, as shown in figure (9a). It was observed that the semicircle diameters increased with higher concentrations of Glimepiride. The slight deviation from a perfect arc may have been caused by the effects of grain boundaries, surface irregularities, and residual contaminants on CS [55]. Furthermore, the addition of Glimepiride led to an increase in charge transfer resistance (R_{ct}) values and a decrease in capacitance double-layer (C_{dl}) values, indicating the development of a shielding film on the external layer of CS [56]. The EIS data and Cdl values were calculated using Eq. (11) and (12) and were recorded in table 9.

$$C_{dl} = Y_o(\omega_{max})^{n-1} \quad (11)$$

ω_{max} represents the angular frequency related to the frequency of the applied AC signal [57].

Double-layer capacitance given by:

$$C_{dl} = \epsilon\epsilon_0 \left(\frac{A}{\delta}\right) \quad (12)$$

ϵ is the dielectric constant of the electrolyte, δ is the distance between the charged layer, A is electrode surface area and ϵ_0 is the electric constant ($8.854 \times 10^{-12}\text{F/m}$)

while Bode plot consists of two parts:

1. $|Z|$ vs. log f (magnitude of impedance vs. frequency)
2. Phase angle ($^\circ$) vs. log f (magnitude of impedance vs. frequency)

From a corrosion inhibition point of view, these two features help evaluate:

- Barrier properties of the inhibitor film.
- Capacitive behavior of the metal surface (due to adsorption of inhibitor).
- Resistance to charge transfer during corrosion.

Figure (9b) shows that the addition of Glimepiride increases both impedance magnitude ($|Z|$) and phase angle, especially at low and intermediate frequencies. This indicates improved corrosion resistance due to the formation of a protective layer on the (CS) surface. The higher $|Z|$ values reflect reduced charge

transfer, while the increased phase angle suggests enhanced capacitive behavior. These results confirm that Glimepiride effectively inhibits corrosion by forming a stable protective layer that impedes charge transfer processes on the (CS) surface., consistent with other electrochemical and weight loss findings.

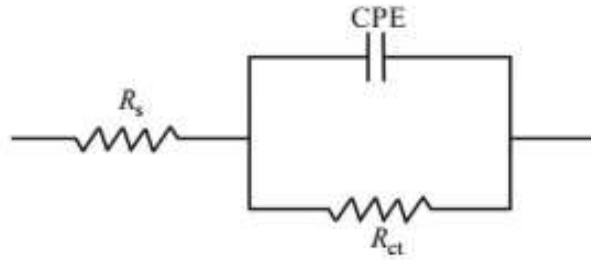


Figure 8 circuit model graph utilized for representing EIS measurements.

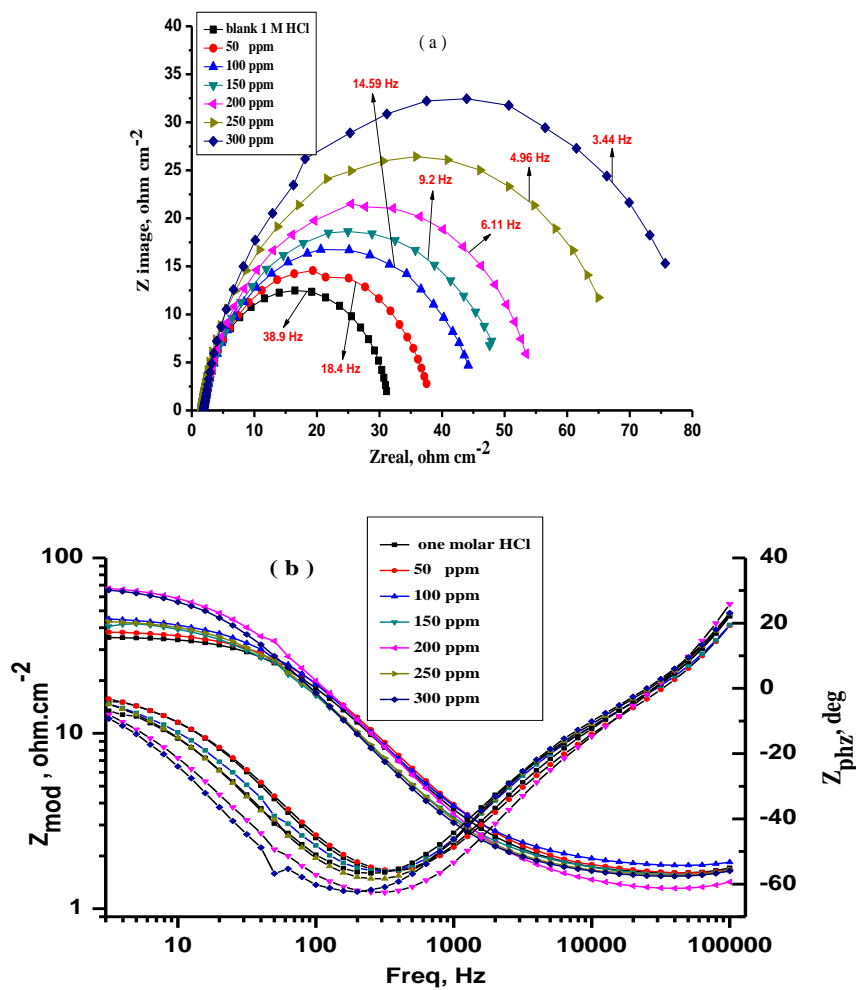


Figure 9: (CS) degradation in degradative acid solution EIS spectra, (a) Nyquist and (b) Bode graph both without plus with Glimepiride varying concentration.

Table 9: carbon steel degradation in degradative acid solution EIS values both without plus with Glimepiride varying concentration.

Concentration ppm	RS, cm ²	Y _o , μΩ ⁻¹ s ⁿ cm ⁻²	n	R _{ct} , Ωcm ²	Cdl, μFcm ⁻²	θ	IE%
0	1.90	326	0.970	29	284.4	-----	-----
50	1.62	284	0.889	43.3	164.1	0.330	33.0
100	1.76	260	0.883	48.1	145.5	0.395	39.5
150	1.52	232	0.881	56.3	128.4	0.484	48.4
200	1.51	225	0.875	62.1	122.1	0.532	53.2
250	1.92	214	0.870	77.7	116.0	0.626	62.6
300	1.72	196	0.868	89.4	105.7	0.675	67.5

3.2.3. EFM PROCESSES

A method that prevents damage, quickly and accurately evaluates the deterioration of carbon steel in its surroundings, regardless of polarization trends. The accuracy of EFM measurements was confirmed using causality factors. Figure 10 illustrates the EFM spectrum, showing the relationship between current and frequency. The concentration of Glimepiride had a direct impact on the increase in IE%. The values of causality coefficients (CF-2 & CF-3) closely aligned with their theoretical benchmarks, demonstrating the high reliability of the recorded values [58]. Table 10 contains electrochemical data on carbon steel degradation in a corrosive acidic solution, both with and without varying concentrations of Glimepiride.

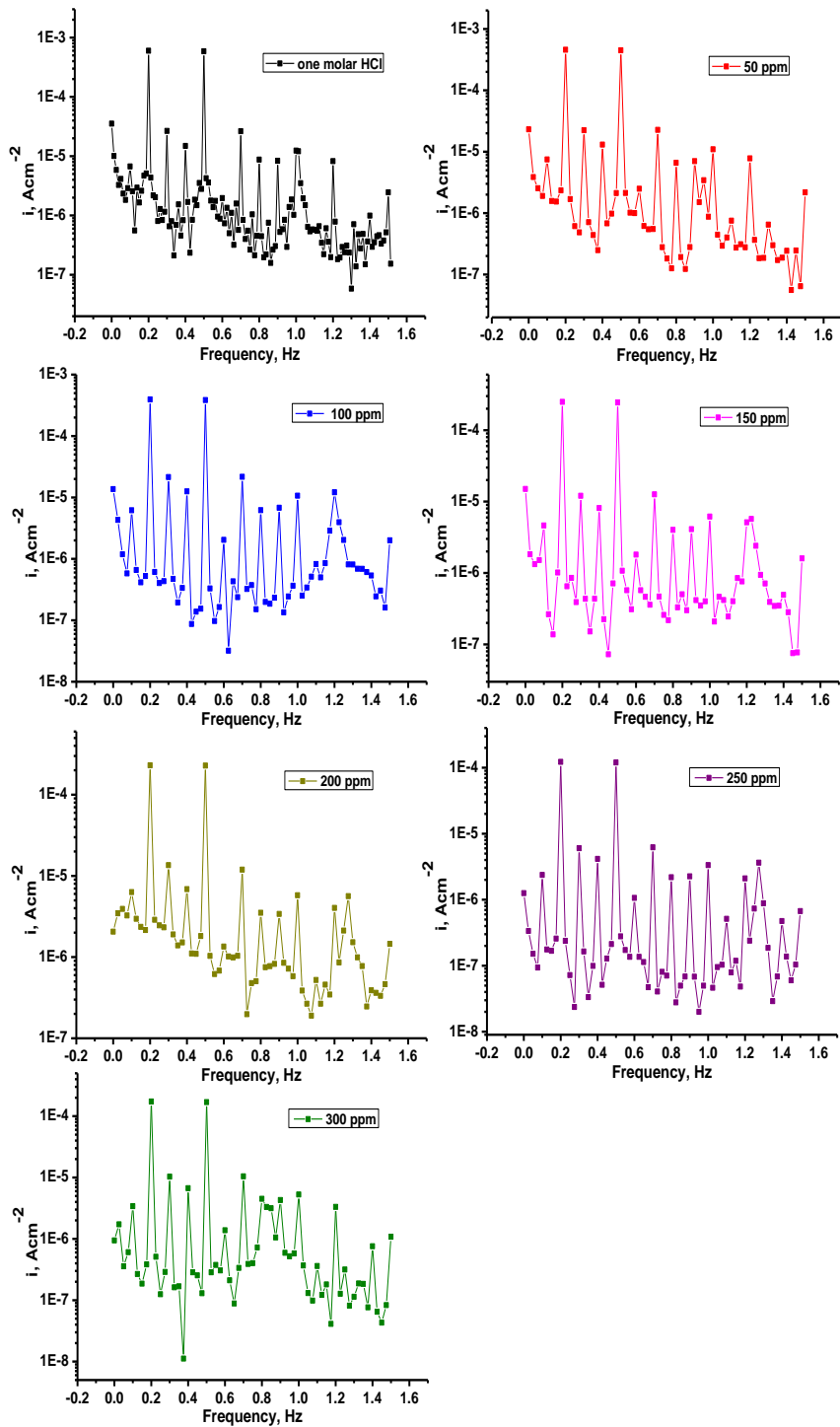


Figure 10: carbon steel degradation in degradative acid solution EFM spectra both without plus with Glimepiride varying concentration.

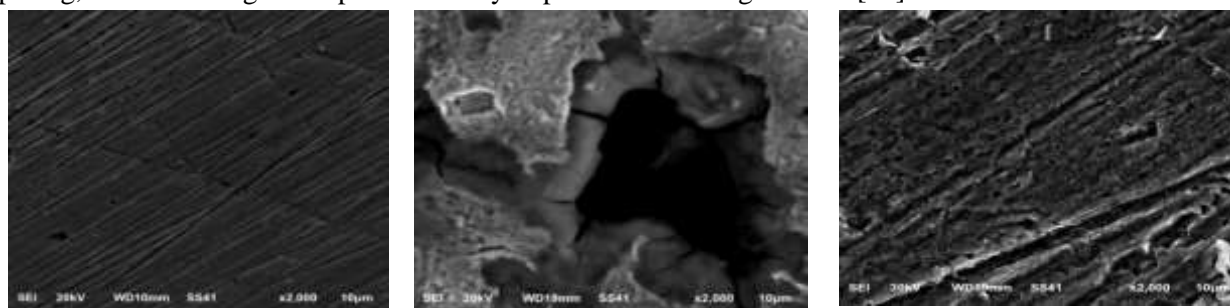
Table 10: Electrochemical parameters from EFM of the CS in 1.0 M HCl both without plus with various doses of Glimepiride compound at 298K

Concentration n Ppm	i_{corr} , μAcm^{-2}	$-\beta_c$, $mVdec^{-1}$	β_a , $mVdec^{-1}$	CF- 2	CF- 3	k_{corr} , mpy	θ	%IE
0	929	191	135	1.8	3.5	480	-----	-----
50	643.7	108	81	1.7	3.0	336.85	0.328	32.8
100	480	111	85	1.7	3.4	250	0.499	49.9
150	323	101	76	1.6	3.0	169.5	0.663	66.3
200	300	103	75	2	2.2	167	0.687	68.7
250	282.9	100	73	1.5	2.9	146.45	0.705	70.5
300	268	91	65	2	3.0	139	0.720	72.0

3.3. SURFACE PROCESSES

3.3.1. SEM PROCESSES

The surface morphologies of carbon steel were observed using SEM after being immersed in one molar hydrochloric acid for 24 hours at 298K. The study compared the effects of high concentration (300 ppm) and without Glimepiride (blank) on the steel surface. Figure 11 shows that the degradative solution caused significant surface damage and pitting, while the presence of Glimepiride resulted in the development of a shielding layer on the carbon steel surface. This layer led to reduced damage and pitting, demonstrating Glimepiride's ability to prevent metal degradation [59].



1

2

3

Figure 11: CS specimens SEM images: (1) uncontaminated CS, (2) CS immersed full day in degradative acid and (3) CS immersed full day in degradative acid plus Glimepiride of optimal concentration.

3.3.2. AFM PROCESSES

The atomic force microscope (AFM) is an excellent tool for examining surface topography and evaluating the effectiveness of corrosion inhibition on carbon steel (CS) after being exposed to a degradative acid, as it produces three-dimensional images of surfaces at the nanoscale to microscale [60]. The three-dimensional AFM images in Figure 12 depict the degradation of carbon steel in a degradative acid, both in the absence and presence of 300 ppm Glimepiride. The surface irregularities, represented by the mean deviation (R_q), and the typical variations across the entire texture measurements (R_a) are

measured. The AFM images of carbon steel in the degradative solution alone reveal significant degradation and increased roughness. Conversely, the inclusion of Glimepiride leads to reduced pitting, indicating the formation of a protective film on the external layer of the CS. The inhibition efficiency (IE %) determined from electrochemical tests and mass reduction tests supports the observed surface texture measurements. The consistency between the roughness data presented in table 11 suggests a less textured surface for CS, indicating the development of a protective film facilitated by Glimepiride.

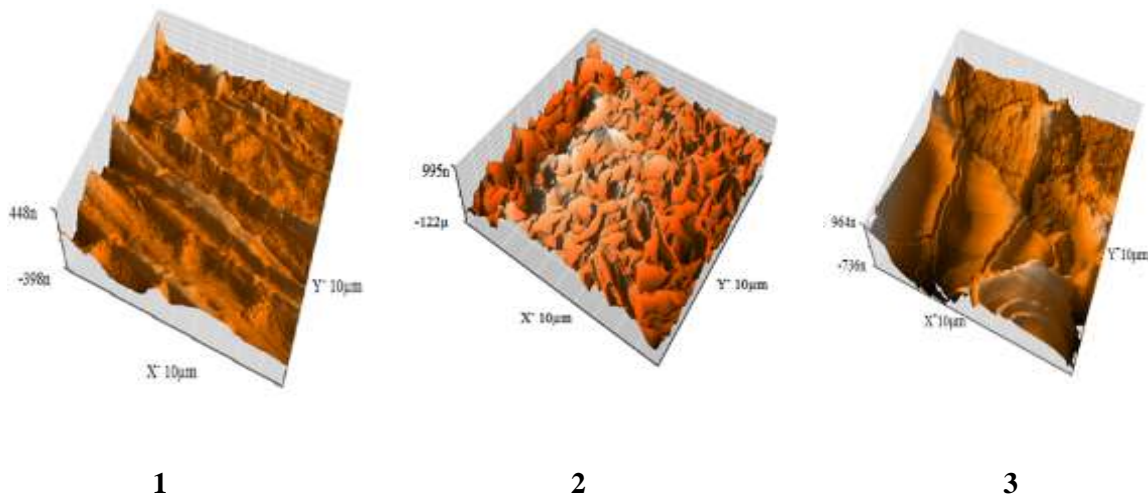


Figure 12: CS specimens AFM scans: (1) before exposure to degradative solution, (2) immersed full day in degradative acid and (3) immersed full day in degradative acid plus Glimepiride of optimal concentration.

Table 11: CS specimens surface texture data involvement plus nonexistence of Glimepiride optimal dose in one molar hydrochloric acid for one-day

Specimen	Average roughness (Ra) nm	RMS roughness (Rq) nm
(CS) metal surface (pure)	48.7	63.0
(CS) metal surface + 1.0 M HCl (blank)	271.7	335.6
(CS) metal surface + Glimepiride	195.1	262.5

3.3.3. FTIR PROCESSES

The approach used to analyze the functional groups of Glimepiride adsorbed on the outer layer of CS is illustrated in Figure 13, which depicts the IR spectral data of Glimepiride. It demonstrates the formation of a protective film on the external layer of CS after a 6-hour immersion in a degradative acid along with an optimal Glimepiride concentration of 300 ppm. The examination of the distinct peaks revealed minor changes, including the disappearance of some functional group frequencies and the shifting of others [61], as detailed in table 12. These alterations are attributed to the chemisorption process, involving the interaction and bonding of Glimepiride with the outer layer of carbon steel. The identified peaks confirm the presence of Glimepiride, indicating that heteroatoms such as O and N act as active sites, protecting CS by forming a protective layer when exposed to a degradative solution on carbon steel [62]. Additionally, the π electrons from double bonds also contribute to this protective effect.

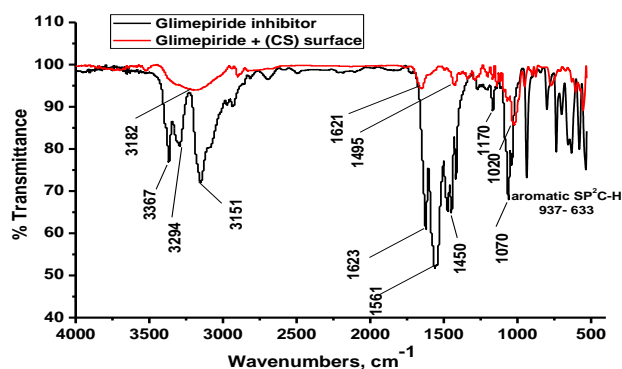


Figure 13: Glimepiride FT-IR spectra alone and with carbon steel after a 6-hour immersion in one molar hydrochloric acid with an optimal Glimepiride concentration 300 ppm.

Table 12: FT-IR analysis of Glimepiride alone and with carbon steel after 6-hour immersion in one molar hydrochloric acid with an optimal Glimepiride concentration 300 ppm.

Peak frequencies (cm ⁻¹)	Functional groups represented by frequencies	Peak shifts, frequency changes and new peaks (cm ⁻¹) observed after adsorption
3367-3294	-NH ₂ primary amine Stretching vibration	3182
3151	SP ² (-C-H) Stretching vibration	Missed
1623	aromatic conjugated (-C=O) amide group	Missed
1450	-N-H- bending vibration	Missed
1561	stretching (C=C)	1495
1070	Alkoxy aliphatic (C-O)	Missed
1170	bending -C-N-	Missed
937-633	bending aromatic SP ² (C-H)	950-554
800	di-substituted in the ortho positions	774
736	di-substituted in the Para positions	711
655	di-substituted in the meta positions	631

3.3.4. XPS PROCESSES

The processes utilized aimed to develop a deeper understanding of the chemical behavior of Glimepiride on the outer layer of CS. Figures 14 and 15 display the CS outer layer after being fully immersed in a degradative acid along with optimal concentration of Glimepiride. XPS profiles data for Fe 2p, O 1s, Cl 2p, C 1s, and N 1s were obtained. The observed complex forms in all XPS spectra were attributed to their corresponding species through a deconvolution fitting process [63–72]. The data analysis measurements were presented in table 13. The XPS spectrum confirmed the formation of a protective film composed of C, O, and N atoms on the outer layer of CS by Glimepiride.

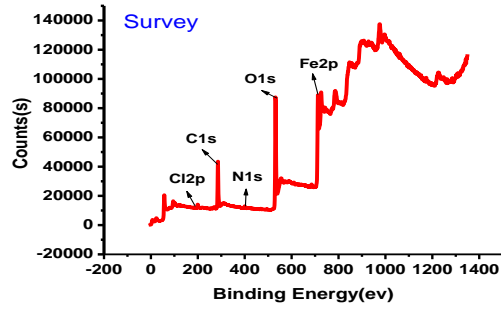


Figure 14: Glimepiride optimal concentration adsorbed upon outer layer of CS XPS spectra in degradative acid.

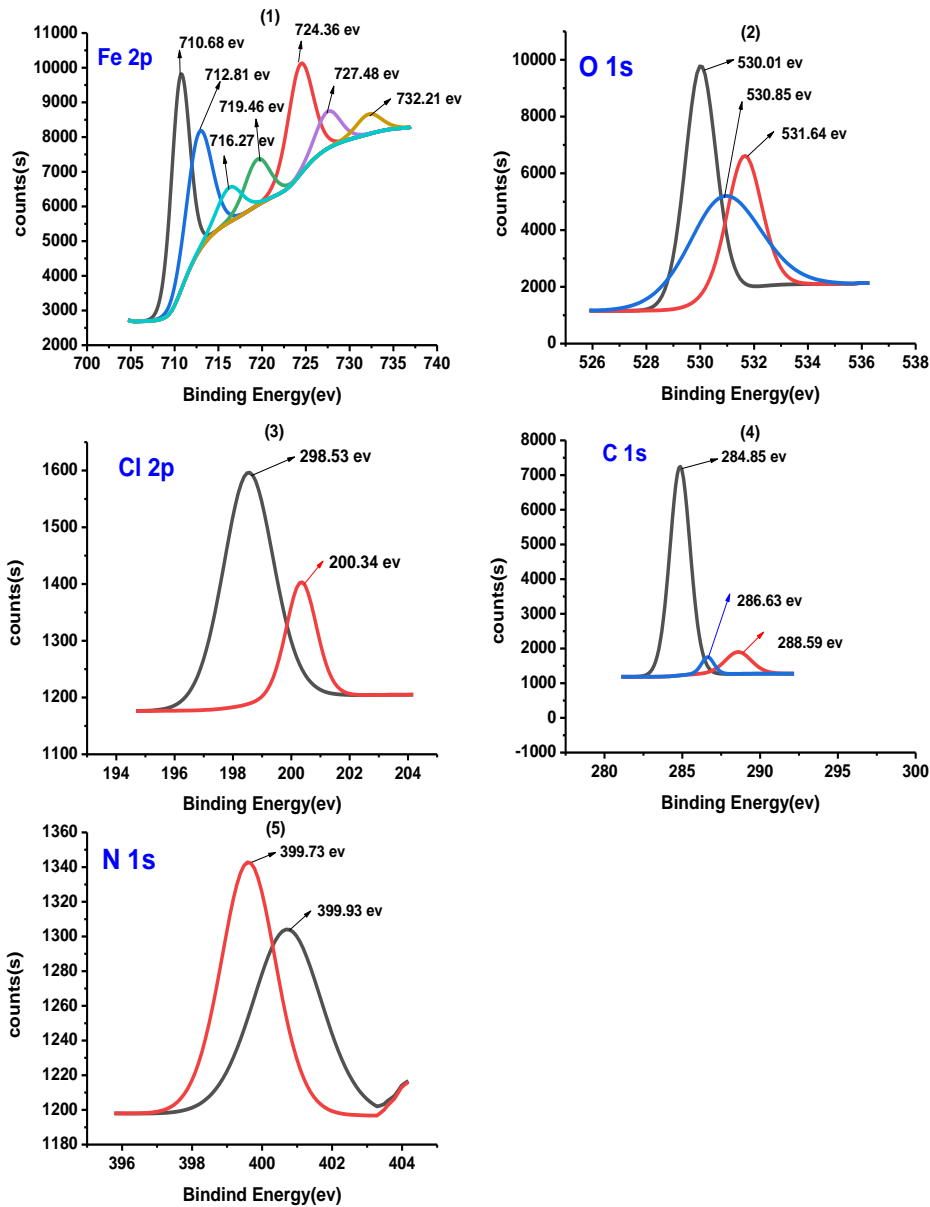


Figure 15: CS post immersed full day in a degradative acid plus Glimepiride of optimal concentration Fe 2p, O 1s, Cl 2p, C 1s, and N 1s XPS profiles data.

Table 13: predicted bonds related to various spectra binding energies lists.

Type of scan	Peaks value of binding energies (eV)	Predicted bonds
Fe 2p	710.68	2p3/2 core level electrons of iron in its +2-oxidation state as found in FeO.
	712.81	2p3/2 core level electrons of iron in its +3-oxidation state as in Fe ₂ O ₃ or FeCl ₃
	716.27	2p3/2 core level electrons of iron in its +2-oxidation state as additional peaks
	719.46	2p3/2 core level electrons of iron in its +3-oxidation state as additional peaks
	724.36	2p1/2 core level electrons of iron in its +2-oxidation state as found in FeO.
	727.48	2p1/2 core level electrons of iron in its +3-oxidation state as found in Fe ₂ O ₃ .
	732.21	2p1/2 core level electrons of iron in its +3-oxidation state as additional peaks
O 1s	530.01	Iron in its +3-oxidation state as found in Fe ₂ O ₃ .
	530.85	Carbon-oxygen single bond
	531.64	Carbonyls shows up slightly higher in energy
Cl 2p	198.53	Chlorine atom in 2p3/2 orbital
	200.34	Chlorine atom in 2p1/2 orbital slightly higher energy
C 1s	284.85	Carbon atoms bonded to each other in aromatic ring.
	286.63	Different carbon bonds with O, N or Cl
	288.58	Carbonyl carbon in amides or similar structures
N 1s	399.73	Imines or other similar compounds
	400.93	Nitrogen-hydrogen single bond

3.4. QUANTUM CHEMICAL AND STATISTICAL PARAMETERS

The relationship between the molecular structure of Glimepiride and its effectiveness in preventing carbon steel degradation is influenced by quantum parameters. Table 14 outlines these parameters. Figure 16 illustrates the distribution of Glimepiride electron concentrations. Higher EHOMO values indicate a greater likelihood of Glimepiride transferring electrons to the vacant d-orbitals of carbon steel, leading to stronger adsorption. Conversely, lower ELUMO values suggest a higher tendency for Glimepiride to accept electrons. The ΔE value reflects the distribution of electron density and the reactivity of molecules. Data on molecular stability and reactivity, denoted as (η) and (σ), is presented in table 14. A higher softness (σ) and lower hardness (η) are generally associated with better inhibition efficiency. The polarity and electron-sharing bonding type of Glimepiride, represented by (μ), are influenced by electron distribution. In general, hard molecules with larger (ΔE) are more resistant to electronic perturbations, while soft molecules with smaller (ΔE) are more reactive and efficient in corrosion inhibition due to their

ease of electron donation. Glimepiride acts as an electron donor, while carbon steel, with its vacant d-orbitals, acts as an electron acceptor[73]

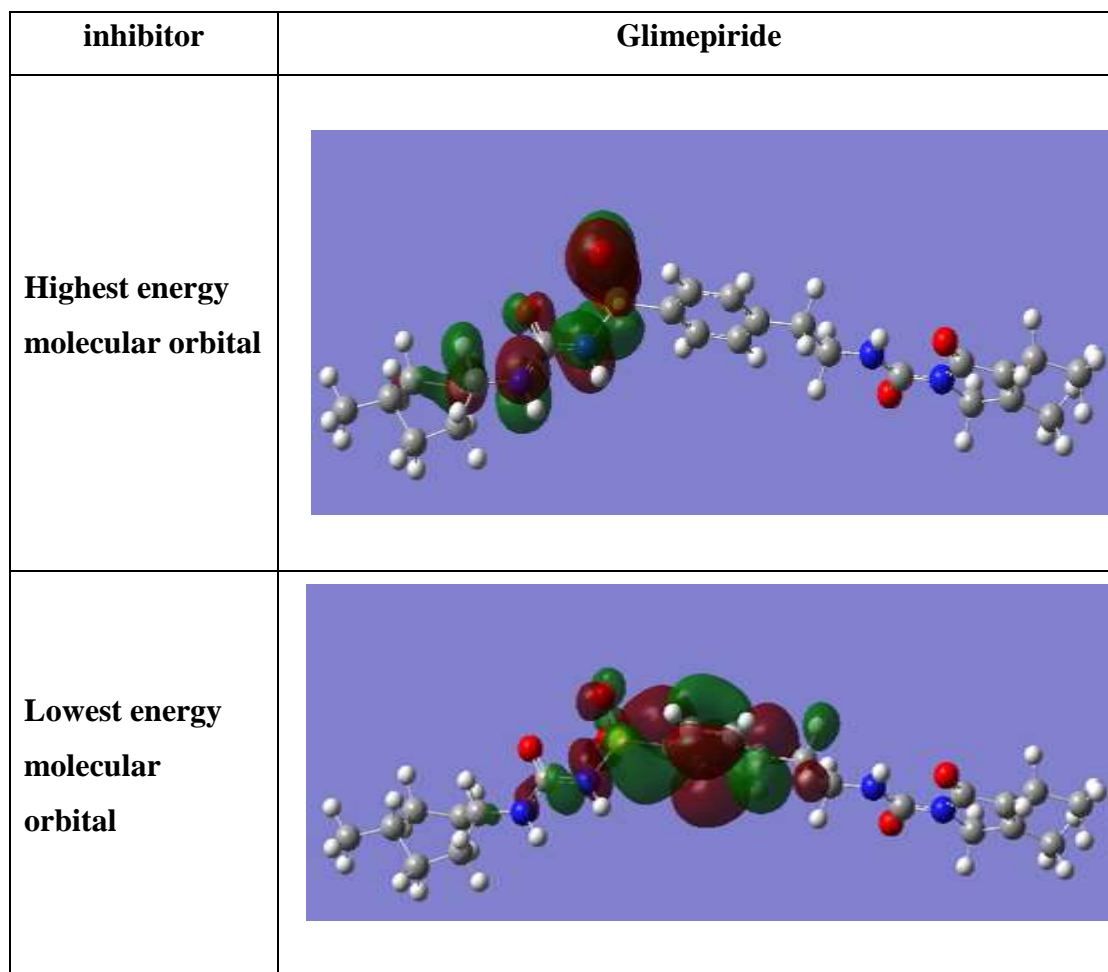


Figure 16: Glimepiride highest energy molecular orbital plus lowest energy molecular orbital electronic densities distributions.

Table 14: Molecular quantum metrics for Glimepiride in solution

Metrics	E_{HOMO} (eV)	E_{LUMO} (eV)	ΔE (eV)	η (eV)	σ (eV)	Π (Ev)	X (eV)	μ (Debye)
Glimepiride	-6.32	-1.91	4.408	2.204	0.453	-4.119	4.119	12.7102

4. MECHANISM OF INHIBITION

The performance of Glimepiride in inhibiting the degradation of CS in acidic conditions was studied. Various factors influence the effectiveness of the inhibition, such as the concentration of Glimepiride, its molecular mass, the charge density, and number of its active sites, as well as its environmental stability [74]. The presence of heteroatoms (N, O, and S) in Glimepiride and their ability to donate electrons play a crucial role in reducing the degradation of carbon steel. The mechanism of inhibition involves the attachment of Glimepiride to the surface of carbon steel, effectively covering its active sites [75]. The

structure of Glimepiride, which contains different electronically active functional groups, helps in forming coordination bonds with the empty d-orbitals of CS, leading to a chemical adsorption process that displaces water molecules adsorbed on the surface of carbon steel, allowing Glimepiride to create a protective barrier against CS degradation.

The effectiveness of the adsorption process depends on the affinity of carbon steel for electron-rich sites, resulting in better surface coverage and improved resistance to degradation [76–78].

The observed differences in inhibition efficiency (IE%) between weight loss and electrochemical methods result from differences in measurement timescales, sensitivity, and experimental conditions. Weight loss represents the total carbon steel loss over time (long period) exposure to the aggressive HCl solution. while Electrochemical methods such as potentiodynamic polarization or electrochemical impedance spectroscopy (EIS) measure the corrosion kinetics and surface response at a specific point in time. Therefore, small differences in IE% between WL and electrochemical methods are expected and acceptable, where they show the same results with increasing glimepiride concentration. As shown in table 15 and figure 17.

Table 15: IE % obtained from weight loss, hydrogen evolution, PP, EIS and EFM measurements for CS in 1.0 M HCl solution of the investigated Glimepiride at 298 K.

Glimepiride	IE%			
	weight loss	pp	EIS	EFM
50	50.6	61.3	33.0	32.8
100	54.6	66.8	39.5	49.9
150	58.2	67.7	48.4	66.3
200	61.6	75.6	53.2	68.7
250	63.4	77.2	62.6	70.5
300	66.1	79.4	67.5	72.0

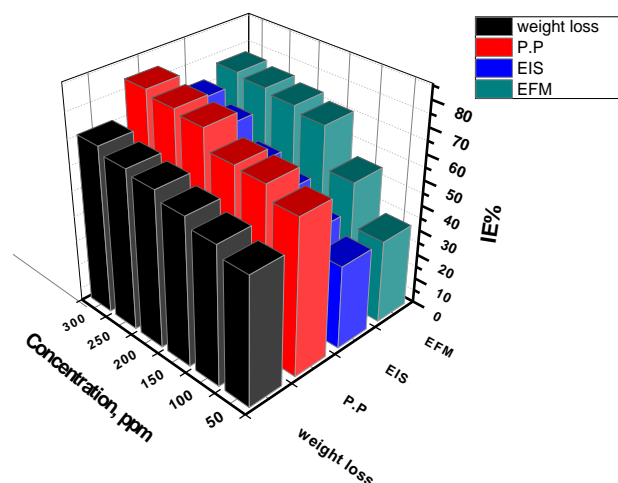


Figure 17: Comparison of the inhibition efficiencies (IE%) values from different studied techniques for CS in 1.0 M HCl solution of the investigated Glimepiride at 298 K.

5. CONCLUSION

Glimepiride effectively decreases the carbon steel degradation in the corrosive solution. The adsorption of Glimepiride is represented by the Temkin isotherm. Higher solution temperatures and greater Glimepiride concentration result in an increased IE%, indicating chemical adsorption of Glimepiride on the outer layer of CS. Potentiodynamic data shows that Glimepiride acts as a mixed inhibitor. EIS data reveals that, the double layer capacitance decreases progressively due to the formation of a protective shield against degradation on the external layer of CS, which is not observed in the absence of Glimepiride. The measured data obtained from electrochemical, non-electrochemical, and surface examinations can be considered as confirming each other.

6. REFERENCES

- [1] L. T. Popoola, Organic green corrosion inhibitors (OGCIs): a critical review, *Corrosion Reviews*, 37 (2019) 71-102.
- [2] A. O. Gadioli, L. M. de Souza, E. C. Pereira, S. N. Monteiro, and A. R. Azevedo, Imidazolium-based ionic liquids as corrosion inhibitors for stainless steel in different corrosive media: An overview, *J. Mat. Res. Tech.* (2024).
- [3] B. Yin, N. Josselyn, T. Considine, J. Kelley, B. Rinderspacher, R. Jensen and E. Rundensteiner, Corrosion image data set for automating scientific assessment of materials. In *British Machine Vision Conference (BMVC)*, (2021) 1-15.
- [4] S. Z. Salleh, A. H. Yusoff, S. K. Zakaria, M. A. A. Taib, A. A. Seman, M. N. Masri and P. Ter Teo, Plant extracts as green corrosion inhibitor for ferrous metal alloys: A review, *J. Clean. Prod.* 304 (2021) 127030.
- [5] R. Aslam, M. Mobin, S. Zehra, and J. Aslam, A comprehensive review of corrosion inhibitors employed to mitigate stainless steel corrosion in different environments, *J. Mol. Liq.*, (2022) 119992.
- [6] Q. Mohsen and M. A. Deyab, Utilizing birch leaf extract in pickling liquid as a sustainable source of corrosion inhibitor for pipeline steel, *Scientific Reports*, 12 (2022) 19307.
- [7] R. Hernández-Bravo, A. D. Miranda, J. G. Parra, J. M. Alvarado-Orozco, J. M. Domínguez-Esquível, and V. Mujica, Experimental and theoretical study on the effectiveness of ionic liquids as corrosion inhibitors. *Computational and Theoretical Chemistry*, 1210 (2022) 113640.
- [8] V. Gentil, L. Carvalho, *Corrosão Grupo GEN* (2022) 408 7th ed.
- [9] M. M. Solomon, S. A. Umoren, M. A. Quraishi, D. B. Tripathy and E.J. Abai, Effect of alkyl chain length, flow, and temperature on the corrosion inhibition of carbon steel in a simulated acidizing environment by an imidazoline-based inhibitor, *J. Petrol. Sci. Eng.* 187 (2020) 106801.
- [10] P. Pillai, M. Maiti and A. Mandal, Mini-review on recent advances in the application of surface-active ionic liquids: petroleum industry perspective, *Energy Fuel*, 36 (2022) 7925-7939.
- [11] O. Dagdag, An overview of corrosion Anticorrosive Nanomaterials: Future perspectives, 56 (2022) 44.
- [12] A. Allahyarzadeh-Bidgoli, L. O. Salviano, D. J. Dezan, S. de Oliveira Junior and J. I. Yanagihara, Energy optimization of an FPSO operating in the Brazilian Pre-salt region *Energy*, 164 (2018) 390-399.
- [13] T. K. Sarkar, M. Yadav and I. B. Obot, Mechanistic evaluation of adsorption and corrosion inhibition capabilities of novel indoline compounds for oil well/tubing steel in 15% HCl, *Chem. Eng. J.* 431 (2022) 133481.
- [14] B. H. Shin, J. Park, J. Jeon, S. B. Heo and W. Chung, Effect of cooling rate after heat treatment on pitting corrosion of super duplex stainless steel UNS S 32750, *Anti-corrosion Methods and Mater.* 65 (2018) 492-498.

- [15] S. Znaniecki, K. Szwabińska, J. Wojciechowski, A. Skrzypczak and G. Lota, Ionic liquid modified electrochemical capacitor with long-term performance *Chemelectrochem*, 8 (2021) 3685-3694.
- [16] F. R. Kashani and M. Rezaei, Improving the localized corrosion resistance of 304 stainless steel in HCl solution by adsorption of molybdate ions: interaction mechanisms at the interface using molecular dynamics simulation and electrochemical noise analysis, *Colloids Surf. A Physicochem Eng. Asp*, 647 (2022) 129085.
- [17] F. Simescu-Lazar, S. Slaoui, M. Essahli, F. Bohr, A. Lamiri, L. Vanoye and J. P. Chopart, Thymus satureoides oil as green corrosion Inhibitor for 316L stainless steel in 3% NaCl: experimental and theoretical studies, *Lubricants*. 11 (2023) 56.
- [18] A. Sh Nahlé, R. Salim, F. E. Hajjaji, E. Ech-Chihbi, A. Titi, M. Messali, S. Kaya, B. El Ibrahimy and M. Taleb, Experimental and theoretical approach for novel imidazolium ionic liquids as Smart Corrosion inhibitors for mild steel in 1.0 M hydrochloric acid, *Arab J. Chem*, 15 (2022) 103967.
- [19] M. Abdallah, M. A. Hegazy, M. Alfakeer and H. Ahmed, Adsorption, and inhibition performance of the novel cationic Gemini surfactant as a safe corrosion inhibitor for carbon steel in hydrochloric acid, *Green Chem Lett Rev*, 11 (2018) 457-468.
- [20] R. Salim, E. Ech-Chihbi, H. Oudda, F. El Hajjaji, M. Taleb and S. Jodeh, A review on the assessment of imidazo [1, 2-a] pyridines as corrosion inhibitor of metals, *Journal of Bio-and Tribo-Corrosion*, 5 (2019) 1-10.
- [21] E. K. Ardakani, E. Kowsari, A. Ehsani and S. Ramakrishna, Performance of all ionic liquids as the eco-friendly and sustainable compounds in inhibiting corrosion in various media: a comprehensive review, *Microchem J*. 165 (2021) 106049.
- [22] M. Zunita and Y. J. Kevin, Ionic liquids as corrosion inhibitor: from research and development to commercialization, *Results in Engineering* (2022) 100562.
- [23] F. E. Hajjaji, E. Ech-Chihbi, R. Salim, A. Titi, M. Messali, B. El Ibrahimy, S. Kaya, and M. Taleb, A detailed electronic-scale DFT modeling/MD simulation, electrochemical and surface morphological explorations of imidazolium-based ionic liquids as sustainable and non-toxic corrosion inhibitors for mild steel in 1 M HCl, *Mater Sci Eng, B*, 289 (2023) 116232.
- [24] M. A. Deyab, Understanding the anti-corrosion mechanism and performance of ionic liquids in desalination, petroleum, pickling, de-scaling, and acid cleaning applications, *J. Mol. Liq.* 309 (2020) 113107.
- [25] H. S. Lee, V. Saraswathy, S. J. Kwon and S. Karthick, Corrosion inhibitors for reinforced concrete: a review. *Corrosion inhibitors, principles, and recent applications*, (2018) 95-120.
- [26] P. Arellanes-Lozada, V. Díaz-Jiménez, H. Hernández-Cocolezzi, N. Nava, O. Olivares-Xometl and N. V. Likhanova, Corrosion inhibition properties of iodide ionic liquids for API 5L X52 steel in acid medium, *Corros. Sci.* 175 (2020) 108888.
- [27] C. Verma, E. E. Ebenso, M. A. Quraishi and C. M. Hussain, Recent developments in sustainable corrosion inhibitors: design, performance and industrial scale applications, *Materials Advances*, 2 (2021) 3806-3850.
- [28] M. Yeganeh, I. Khosravi-Bigdeli, M. Eskandari and S. R. Alavi Zaree, Corrosion inhibition of L-methionine amino acid as a green corrosion inhibitor for stainless steel in the H₂SO₄ solution, *J. Mater Eng Perform.* 29 (2020) 3983-3994.
- [29] G. A. Swetha and H. P. Sachin, Evaluation of the effectiveness of gabapentin as a corrosion inhibitor for mild steel in a 1 M hydrochloric acid environment using theoretical and experimental methods, *Inorg. Chem. Commun*, 155 (2023) 111082.
- [30] O. S. Shehata, L. A. Korshed and A. Attia, Green corrosion inhibitors, past, present, and future *Corrosion inhibitors, principles, and recent applications* (2018) 121.
- [31] Q. Wang, B. Tan, H. Bao, Y. Xie, Y. Mou, P. Li, D. Chen, Y. Shi, X. Li and W. Yang, Evaluation of *Ficus tikoua* leaves extract as an eco-friendly corrosion inhibitor for carbon steel in HCl media, *Bioelectrochemistry*, 128 (2019) 49-55.
- [32] A. Simović, S. Stevanović, B. Milovanović, M. Etinski and J. B. Bajat, Green corrosion inhibitors of steel based on peptides and their constituents: a combination of experimental and computational approach, *J. Solid State Electrochem* (2023) 1-14.

- [33] A. S. Fouda, A. A. Ibrahim and W. T. El-behairy, Thiophene derivatives as corrosion inhibitors for carbon steel in hydrochloric acid solutions, *Scholars Research Library* 6 (2014) 144-157.
- [34] S. M. Shaban, I. Aiad, M. M. El-Sukkary, E. A. Soliman and M. Y. El-Awady, Evaluation of some cationic surfactants based on dimethylaminopropylamine as corrosion inhibitors, *J. Ind. Eng. Chem.* 21 (2015) 1029–1038.
- [35] F. Bentiss, M. Lagrenee, M. Traisnel and J. C. Hornez, The corrosion inhibition of mild steel in acidic media by a new triazole derivative, *Corros. Sci.* 41 (1999) 789-803.
- [36] I. Ahamad and M. A. Quraishi, Bis (benzimidazol-2-yl) disulphide: An efficient water-soluble inhibitor for corrosion of mild steel in acid media, *Corros. Sci.* 51 (2009) 2006–2013.
- [37] S. S. Abdel-Rehim, K. F. Khaled and N. S. Abd-Elshafi, Electrochemical frequency modulation as a new technique for monitoring corrosion inhibition of iron in acid media by new thiourea derivative, *Electrochimica Acta* 51 (2006) 3269–3277.
- [38] B. Delley, From molecules to solids with the DMol 3 approach, *The J. Chem. Phys.* 113 (2000) 7756-7764.
- [39] R. Solmaz, Investigation of adsorption and corrosion inhibition of mild steel in hydrochloric acid solution by 5-(4-Dimethylaminobenzylidene) rhodanine, *Corros. Sci.* 79 (2014) 169-176.
- [40] D. D. N. Singh, R. S. Chaudhary, B. Prakash and C. V. Agarwal, Inhibitive efficiency of some substituted thioureas for the corrosion of aluminium in nitric acid, *Bri. Corros. J.* 14 (1979) 235-239.
- [41] K. Sudhish and M. A. Quraishi, Sh., 4-Substituted anilinomethylpropionate: new and efficient corrosion inhibitors for mild steel in hydrochloric acid solution, *Corros. Sci.* 51 (2009) 1990-1997.
- [42] A. S. Fouda, A. A. Al-Sarawy and E. E. El-Katori, Pyrazolone derivatives as corrosion inhibitors for C-steel in hydrochloric acid solution, *Des.* 201 (2006) 1-13.
- [43] Sh. Masroor and M. Mobin, Non-Ionic Surfactant as Corrosion Inhibitor for Aluminium in 1 M HCl and Synergistic Influence of Gemini Surfactant, *Chem. Sci. Rev. Lett.* 3 (2014) 33-48.
- [44] A. Zarrouk, B. Hammouti, H. Zarrok, S. S. Al-Deyab, and M. Messali, Temperature effect, activation energies and thermodynamic adsorption studies of L-cysteine methyl ester hydrochloride as copper corrosion inhibitor in nitric acid 2M., *International Journal of Electrochemical Science*, 6(12), (2011) 6261-6274.
- [45] S. Masroor, and M. Mobin, Non-ionic surfactant as corrosion inhibitor for aluminium in 1 M HCl and synergistic influence of Gemini surfactant. *Chem. Sci. Rev. Lett.* 3(11S), (2014) 33-48.
- [46] A. Zarrouk, I. Warad, B. Hammouti, A. Dafali, S. S. Al-Deyab, and N. Benchat, The effect of temperature on the corrosion of Cu/HNO₃ in the presence of organic inhibitor: part-2. *International Journal of Electrochemical Science*, 5(10), (2010) 1516-1526.
- [47] B. Hammouti, A. Zarrouk, S. S. Al-Deyab, and L. Warad, Temperature Effect, Activation Energies and Thermodynamics of Adsorption of ethyl 2-(4-(2-ethoxy-2-oxoethyl)-2-p-Tolylquinoxalin-1 (4H)-yl) Acetate on Cu in HNO₃. *Oriental Journal of Chemistry*, 27(1), (2011) 23.
- [48] O. Sanni, A. P. I. Popoola, and O. S. L. Fayomi, Temperature effect, activation energies and adsorption studies of waste material as stainless steel corrosion inhibitor in sulphuric acid 0.5 M. *Journal of Bio-and Tribo-Corrosion*, 5(4), (2019) 88.
- [49] A. M. El-desoky, A. S. Fouda and A. Nabih, Inhibitive, adsorption, synergistic studies on copper corrosion in nitric acid solutions by some organic derivatives, *Adv. Mater. Corros.* 2 (2013) 1-15.
- [50] S. G. Lakshmi, S. Tamilselvi, N. Rajendran, M. A. K. Babi and D. Arivuoli, Electrochemical behaviour and characterisation of plasma nitrided Ti–5Al–2Nb–1Ta orthopaedic alloy in Hanks solution, *Sur. Coat. Tech.* 182 (2004) 287-293.
- [51] Li. Xianghong, D. Shuduan, Mu. Guannan and Y. Fazhon, Inhibition effect of nonionic surfactant on the corrosion of cold rolled steel in hydrochloric acid, *Corros. Sci.* 50 (2008) 420- 430.
- [52] A. S. Fouda, D. Mekkia and A. H. Badr, Extract of *Camellia sinensis* as green inhibitor for the corrosion of mild steel in aqueous solution, *J. Kor. Chem. Soci.* 57 (2013) 264-271.
- [53] M. Abdallah, Rhodanine azosulpha drugs as corrosion inhibitors for corrosion of 304 stainless steel in hydrochloric acid solution, *Corros. Sci.* 44 (2002) 717-728.

- [54] I. Ahamad, R. Prasad, and M. A. Quraishi, Thermodynamic, electrochemical and quantum chemical investigation of some Schiff bases as corrosion inhibitors for mild steel in hydrochloric acid solutions, *Corros. Sci.* 52 (2010) 933-942.
- [55] M. El Achouri, S. Kertit, H. M. Gouttaya, B. Nciri, Y. Bensouda, L. Perez, M. Infante, and K. Elkacemi, Corrosion inhibition of iron in 1 M HCl by some gemini surfactants in the series of alkanediyl- α,ω -bis-(dimethyl tetradecyl ammonium bromide). *Prog in Org Coat* 43 (2001) 267–273.
- [56] A. P. Hanza, R. Naderi, E. Kowsari and M. Sayebani, Corrosion behavior of mild steel in H₂SO₄ solution with 1,4-di [1'-methylene-3'-methyl imidazolium bromide]-benzene as an ionic liquid. *Corros Sci* 107(2016) 96-106.
- [57] S. F. Mertens, C. Xhoffer, B. C. Decooman and E. Temmerman, Short-term corrosion of polymer-coated 55% Al-zn- part 1: behavior of thin polymer films. *Corrosion* 53 (1997) 381- 388.
- [58] E. A. Noor and A. H. Al-Moubaraki, Thermodynamic study of metal corrosion and inhibitor adsorption processes in mild steel/1-methyl-4[4'(-X)-styrylpyridinium iodides/hydrochloric acid systems. *Mater Chem Phys* 110 (2008)145-154.
- [59] R. A. Prabhu, T. V. Venkatesha, A. V. Shanbhag, G. M. Kulkarni, and R. G. Kalkhambkar, Inhibition effects of some Schiff's bases on the corrosion of mild steel in hydrochloric acid solution, *Corros. Sci.* 50 (2008) 3356-3362.
- [60] Y. Tang, X. Yang, W. Yang, Y. Chen, and R. Wan, Experimental, and molecular dynamics studies on corrosion inhibition of mild steel by 2-amino-5-phenyl-1, 3, 4-thiadiazole, *Corros. Sci.* 52 (2010) 242-249.
- [61] G. A. Caignan, S. K. Metcalf, and E. M. Holt, Thiophene substituted dihydropyridines, *J. chem. crys.* 30 (2000) 415-422.
- [62] R. Kamaraj, P. Ganesan, J. Lakshmi and S Vasudevan, Removal of copper from water by electrocoagulation process-effect of alternating current (AC) and direct current (DC), *Environmental Science and Pollution Research*, 20 (2013) 399-412
- [63] K. Boumhara, M. Tabyaoui, C. Jama and F. Bentiss, Artemisia Mesatlantica essential oil as green inhibitor for carbon steel corrosion in 1 M HCl solution: Electrochemical and XPS investigations, *J. Ind. Eng. Chem.* 29 (2015) 146-155.
- [64] V. S. Sastri, M. Elboudjaini, J. R. Brown and J. R. Perumareddi, Surface analysis of inhibitor films formed in hydrogen sulfide medium, *Corrosion* 52 (1996) 447-452.
- [65] N. El Hamdani, R. Fdil, M. Tourabi, C. Jama and F. Bentiss, Alkaloids extract of Retama monosperma (L.) Boiss. Seeds used as novel eco-friendly inhibitor for carbon steel corrosion in 1 M HCl solution: Electrochemical and surface studies, *App. Surf. Sci.* 357 (2015) 1294-1305.
- [66] X. Gao, S. Liu, H. Lu, F. Gao and H. Ma, Corrosion inhibition of iron in acidic solutions by monoalkyl phosphate esters with different chain lengths, *Ind. Eng. Chem. Res.* 54 (2015) 1941–1952
- [67] M. J. Goldberg, J. G. Clabes and C. A. Kovac, Metal-polymer chemistry. II. Chromium-polyimide interface reactions and related organometallic chemistry, *J. Vacc. Sci. Techno. A* 6 (1988) 991–996
- [68] T. Gu, Z. Chen, X. Jiang, L. Zhou, Y. Liao, M. Duan, H. Wang and Q. Pu, Synthesis, and inhibition of N-alkyl-2-(4-hydroxybut-2-ynyl) pyridinium bromide for mild steel in acid solution: Box–Behnken design optimization and mechanism probe, *Corros. Sci.* 90 (2015) 118-132.
- [69] B. Senthilvadivu, V. Aswini and K. Santhosh Kumar, Anti-corrosive behavior of ethanolic extract of banana peel against acidic media and their thermodynamic studies. *Int. J. Sci.* 6 (2007) 1762-1768
- [70] M. Yadav, S. Kumar, R. R. Sinha, I. Bahadur, and E. E. Ebenso, New pyrimidine derivatives as efficient organic inhibitors on mild steel corrosion in acidic medium: Electrochemical, SEM, EDX, AFM and DFT studies, *Journal of Molecular Liquids* 211 (2015) 135-145.
- [71] T. Gu, Z. Chen, X. Jiang, L. Zhou, Y. Liao, M. Duan and Q. Pu, Synthesis, and inhibition of N-alkyl-2-(4-hydroxybut-2-ynyl) pyridinium bromide for mild steel in acid solution: Box–Behnken design optimization and mechanism probe. *Corros. Sci.* 90 (2015) 118–132.

- [72] A. Meneguzzi, C. A. Ferreira, M. C. Pham, M. Delamar and P. C. Lacaze, Electrochemical synthesis, and characterization of poly (5- amino-1-naphthol) on mild steel electrodes for corrosion protection. *Electrochim Acta* 44 (1999) 2149–2156.
- [73] J. Zhang, X. L. Gong, H. H. Yu and M. Du, The inhibition mechanism of imidazoline phosphate inhibitor for Q235 steel in hydrochloric acid medium. *Corros. Sci.* 53 (2011) 3324–3330.
- [74] M. K. Awad, M. S. Metwally, S. A. Soliman, A. A. El-Zomrawy and M. A. bedair, Experimental and quantum chemical studies of the effect of polyethylene glycol as corrosion inhibitors of aluminum surface, *J. Ind. Eng. Chem.* 20 (2014) 796–808.
- [75] H. Ashassi-Sorkhabi, B. Shaabani and D. Seifzadeh, Effect of some pyrimidinic Schiff bases on the corrosion of mild steel in hydrochloric acid solution, *Electrochim. act.* 50 (2005) 3446- 3452.
- [76] S. M. Shaban, Studying the effect of newly synthesized cationic surfactant on silver nanoparticles formation and their biological activity, *J. Mol. Liq.* 216 (2016) 137-145.
- [77] N. A. Negm and S. M. Morsy, Corrosion inhibition of triethanolammonium bromide mono-and dibenzoate as cationic inhibitors in acidic medium, *J. surf. det.* 8 (2005) 283-287.
- [78] V. S. Sastri and J. R. Perumareddi, Molecular orbital theoretical studies of some organic corrosion inhibitors, *Corros. Sci.* 53 (1997) 617–622. [74] Ashassi-Sorkhabi, H., Shaabani, B. and Seifzadeh, D. Effect of some pyrimidinic Schiff bases on the corrosion of mild steel in hydrochloric acid solution, *Electrochim. act.* 50, 3446- 3452, 2005.